

Soft Ferroelectric Modes in Lead Titanate

G. Shirane, J. D. Axe, and J. Harada

Brookhaven National Laboratory, Upton, New York 11973*

and

J. P. Remeika

Bell Telephone Laboratories, Murray Hill, New Jersey 07974

(Received 26 January 1970)

The ferroelectric phase transition in PbTiO_3 has been investigated by the neutron inelastic scattering technique. As is the case with BaTiO_3 , the soft optic mode at the zone center condenses when the temperature is lowered to the Curie point at 490°C . In contrast to BaTiO_3 , however, the lowest transverse optic modes along $[100]$ are well defined (not overdamped), except for the phonons with very small q values. When this optic branch approaches the acoustic branch near the Curie temperature, effects of the "coupling" are clearly observed. Intensities of the soft modes were measured at several zone centers in the ferroelectric phase. Observed values are in qualitative agreement with calculations based upon the mode motions deduced from the atomic positions in the ferroelectric phase.

I. INTRODUCTION

Lead titanate is one of the perovskite-type ferroelectrics¹ with the Curie temperature at 490°C . The general characteristics of this ferroelectric crystal are expected to be similar to those of the prototype BaTiO_3 . There are, however, a few important differences between the two. First of all, the tetragonal c/a ratio is 1.06 in PbTiO_3 at room temperature and is much larger than 1.01 in BaTiO_3 ; thus the parameters associated with the polar phase, such as the spontaneous polarization and ionic shifts, are considerably larger. This means that the difficulty associated with pseudosymmetric structure determination can be avoided. The crystal structure of tetragonal PbTiO_3 has been established unambiguously.² Second, PbTiO_3 offers a wide temperature range at which the tetragonal phase is stable with noticeable change in pertinent parameters. For example, the c/a ratio changes from 1.02 just below T_C to 1.06 at 22°C . This is in marked contrast to the behavior of BaTiO_3 and KNbO_3 , which exhibit successive transitions to orthorhombic and rhombohedral phases.

Reliable dielectric characteristics of PbTiO_3 crystals became available only recently after high-resistivity single crystals were grown by Remeika and Glass.³ Crystals were grown by a flux method, with small quantities of UO_3 added to the melt in order to produce crystals with high resistivity. The uranium content of the crystals was found to be 0.02–0.04%. The Curie temperature of these crystals, $T_C = (492 \pm 5)^\circ\text{C}$, is essentially the same as that in undoped crystals. The dielectric measurements³ gave

$$\epsilon = C/(T - T_0), \quad (1)$$

with the Curie constant $C = 4.1 \times 10^5$ and $T_0 = 449^\circ\text{C}$. The difference between T_C and T_0 signifies the degree of first-order character of the transition.

The present paper reports a neutron scattering study of the lattice dynamical aspect of this ferroelectric transition at 490°C . Since the soft-mode theory of ferroelectrics was developed by Cochran,⁴ extensive experimental studies have been carried out on several perovskites such as SrTiO_3 , KTaO_3 , and BaTiO_3 . Raman and neutron scattering experiments clearly established the well-defined (undamped) soft modes in SrTiO_3 and KTaO_3 . However, they do not exhibit positive Curie temperatures (and are thus incipient ferroelectrics). The soft modes in BaTiO_3 , the prototype of displacive ferroelectrics, have quite a different character. They are highly damped⁵ and extremely anisotropic.⁶ One may speculate that a high damping constant is associated with a high Curie temperature. Thus it is of considerable interest to study the soft mode in PbTiO_3 . As we shall see later, this crystal turns out to be the first example of ferroelectrics in which, at least away from $q = 0$, the well-defined soft modes were observed in paraelectric as well as in ferroelectric phases.

II. EXPERIMENTAL

Single crystals used in this study were grown by Remeika and Glass³ and have a platelike shape with large areas up to $10 \times 10 \text{ mm}^2$ and thickness between 0.7 and 1.2 mm. At room temperature, most of the crystals contain large areas of c domains which occupy 80–95% of the volume. When heated to the cubic phase above 490°C , they become truly single crystal with a narrow mosaic full width

at half-maximum (FWHM) of less than $5'$. The major part of the neutron measurements was done on a selected crystal with the dimensions $10 \times 10 \times 0.8 \text{ mm}^3$. This crystal was mounted in an oven with the $[1\bar{1}0]$ axis vertical. The temperature was controlled within $\pm 1^\circ\text{C}$. The room-temperature data were collected also on a "composite" assembly of five crystals aligned to give "effective" mosaic of approximately 1° . The total volume of this composite is 0.3 cm^3 .

Inelastic neutron measurements were carried out at the Brookhaven high-flux beam reactor using a triple-axis spectrometer. The standard constant Q or constant E scan was employed. In order to compensate for the small size of available crystals, efficient pyrolytic graphite crystals were used as monochromator and analyzer in the reflection position of (002). These were supplied by Union Carbide Corporation, Carbon Production Division; they have the mosaic width of $21'$ FWHM and the dimensions of $2 \times 1.5 \times 0.1 \text{ (in.}^3\text{)}$. Their maximum reflectivity is 40% at 80 meV and is certainly considerably⁷ higher at the two energies employed: 38 and 14 meV. The latter was used in conjunction with a pyrolytic graphite filter. Collimation of the beam was selected as $20'$ and $40'$ before and after the scattering.

Experimental results described in this paper indicate that pyrolytic graphite crystals are ex-

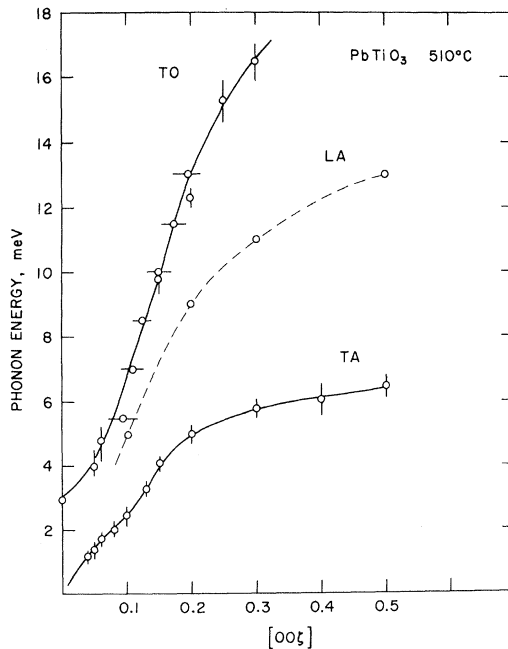


FIG. 1. Three lowest phonon branches in PbTiO_3 at 510°C . Vertical error flags indicate constant Q scans. The dip in the acoustic branch is due to the mode coupling as explained in the text.

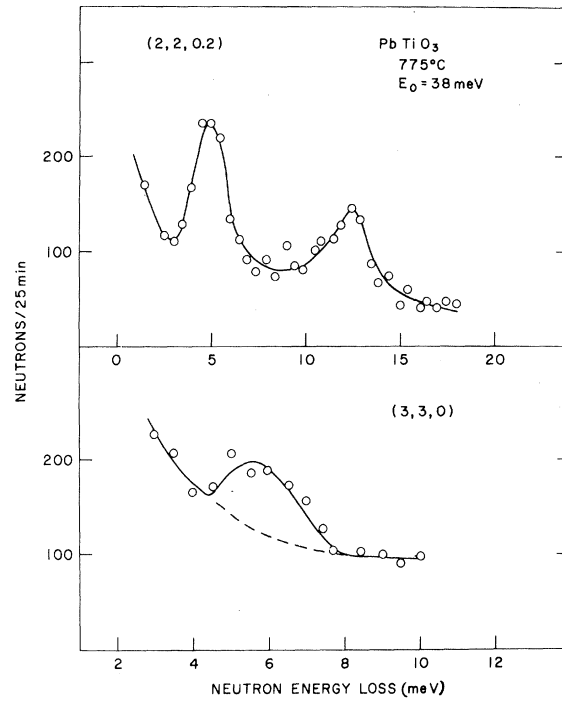


FIG. 2. Representative neutron groups. Data are collected on a small single crystal ($10 \times 10 \times 0.8 \text{ mm}^3$) using pyrolytic graphite monochromator.

tremely useful for special application in neutron inelastic scattering. Crystals with narrow enough mosaic spread (less than 1°) became available only recently. There are severe limitations imposed by the nature of the growth, namely, only hexagonal (00 l) reflections can be used in the reflection position. If one chooses to use (002) reflection, the available energy is probably limited to less than 50 meV. This is conditioned by a small take-off angle for higher-energy neutrons and a larger area required for the monochromator. We consider that 38 meV is a good compromise; *our* pyrolytic graphite (used as both monochromator and analyzer) gives approximately ten times the phonon intensity compared with *our* standard monochromator-analyzer combination, Ge (220) in transmission position.

III. SOFT FERROELECTRIC MODE

The dispersion relation along the $[100]$ direction in cubic PbTiO_3 is shown in Fig. 1. Data are collected at 510°C in the crystal which exhibited the Curie temperature at $(490 \pm 2)^\circ\text{C}$. Examples of representative neutron groups are shown in Fig. 2. In these, the wave vector \vec{q} is represented by the normalized coordinate ξ defined as $\vec{q} = (\xi, 0, 0)a^*$. The soft optic mode was observed at the zone center and its energy increases steeply with increasing

q value. Surprisingly, these soft modes are well defined except for a limited range of small q values with $\zeta < 0.08$. The observed neutron profiles of TO and TA modes with higher ζ can be explained satisfactorily by the resolution of the instrument. The steep slope of this optic branch is very similar to those observed in SrTiO_3 ⁸ and KTaO_3 .⁹ Another important feature in Fig. 1 is a noticeable "dip" in the acoustic mode around $\zeta = 0.1$. This is the result of TA-TO mode interaction and will be discussed in Sec. IV.

The energy of the soft mode at $q = 0$, $\hbar\omega_0$, is expected to follow the following relation:

$$(\hbar\omega_0)^2 = K(1/\epsilon) = A_f(T - T_0) . \quad (2)$$

We encountered some difficulty in measuring the soft-mode energy accurately. The neutron group corresponding to the $q = 0$ mode is rather broad and becomes reasonably well defined only at the highest observation temperature 775 °C as shown in Fig. 2. Only two direct observations were made at $q = 0$ as indicated by open circles in Fig. 3. Another difficulty of the measurement is due to a slow increase of the soft-mode energy with increasing $T - T_0$, in comparison with SrTiO_3 and KTaO_3 . Thus the $q = 0$ optic mode cannot be clearly separated from the background due to low-energy acoustic phonons which are very strong at these elevated temperatures.

There is, however, another method to deduce the $\hbar\omega_0$ by utilizing the relation

$$(\hbar\omega)^2 = (\hbar\omega_0)^2 + \alpha q^2 , \quad (3)$$

where α is the temperature-independent constant. This lattice dynamical expansion was proven to be a good approximation in KTaO_3 ¹⁰ as well as in PbTiO_3 . The energies of the TO branch between $\zeta = 0.08$ and 0.2 can be measured accurately as a function of temperature by constant E scanning. Vertical lines in Fig. 3 were obtained by this extrapolation. The approximate Curie-Weiss law is obeyed with

$$\begin{aligned} (\hbar\omega_0)^2 &= A_f(T - T_0), \quad T_0 = 440 \text{ }^\circ\text{C} , \\ A_f &= 0.13 (\pm 0.03) \text{ meV}^2/\text{ }^\circ\text{C} . \end{aligned} \quad (4)$$

This value of T_0 is in qualitative agreement with the dielectric measurements.³

IV. MODE COUPLING

Recently an extensive study was carried out by Axe *et al.*¹⁰ on the mode coupling when the temperature-dependent optic mode approaches the acoustic mode. By means of a long-wavelength expansion of the lattice dynamical equations, they investigated the effects of harmonic coupling of optic and acousticlike excitations. The most striking feature of this coupling is the anomalous acoustic dispersion, shown as the "dip" in Fig. 1. In centrosymmetric crystals, this interaction vanishes as $q \rightarrow 0$.

Another consequence of this interaction is a remarkable intensity anomaly in the acoustic mode as seen in Fig. 4 for $\zeta = 0.05$. Since the detailed account was given in a recent paper,¹⁰ we may simply remark that a sufficient amount of the optical mode is mixed into the acoustic mode, out of phase, to reduce the intensity. No intensity anomaly was observed for the acoustic mode with $\zeta = 0.20$. The effect of the mixing is, of course, expected to be seen also in the optical branch, although no special effort was made to carry out this more difficult observation.

V. MODE DETERMINATION

Lead titanate is the first example of perovskite-type ferroelectrics for which the soft-mode motion can be compared to the static structure in the tetragonal phase. In BaTiO_3 , the overdamping of the soft mode has made the mode determination extremely difficult. Atomic motions involved in the soft mode have recently been determined¹¹ accurately for SrTiO_3 and KTaO_3 . This study has established the technique so that it can be applied here with sufficient reliability.

At this point, it may be of some interest to examine how the static ferroelectric structures had been interpreted. The structure² of PbTiO_3 at room

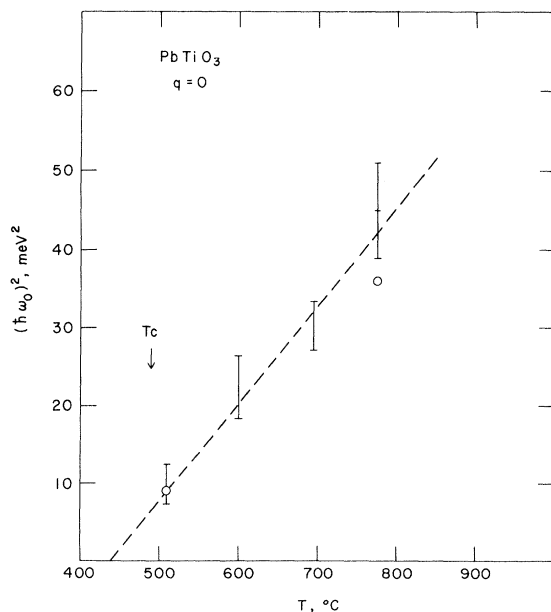


FIG. 3. Soft-mode energy $\hbar\omega_0$ as a function of temperature. Vertical lines represent extrapolation from finite q values as described in the text. Open circles are direct measurements of partially damped mode at $q = 0$.

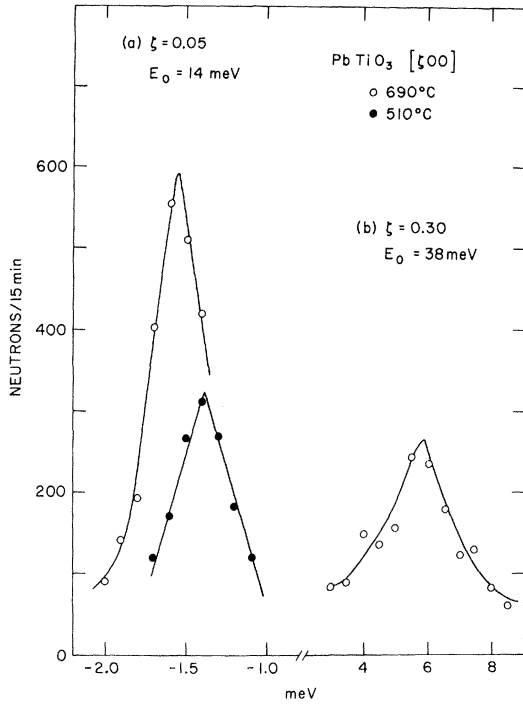


FIG. 4. Phonon profiles for PbTiO_3 (a) shows the mode interaction discussed in the text. Negative energy corresponds to neutron energy $q \cdot r$.

temperature is given in column (I) of Table I. Here the δz 's are "shifts" in fractions of the unit cell. It was argued that the magnitude of these shifts depended on an arbitrary choice of Pb position as the origin; then it might be more natural to refer to the unshifted oxygen octahedron.² There was also an attempt to describe the tetragonal structure in terms of alterations in bond length and angles at the Curie temperature. If we assume that the ferroelectric structure is a simple consequence of the soft-mode condensation,⁴ then there is a unique way to "describe" the structure. It is to apply the simple condition that the center of mass is not displaced, as is required for the $q = 0$ mode [(II) in Table I]. Moreover, as described in Ref. 11, the true normal mode can be approximately decomposed into the two symmetry modes S_1 and S_2 , where S_1 is the Slater mode in which Ti moves against an oxygen octahedron and S_2 corresponds to the motion of Pb against TiO_6 . The soft-mode motion in SrTiO_3 and KTaO_3 is mainly of the S_1 type.¹¹

Intensity distribution of equivalent phonons at total momentum transfer Q at different Brillouin zones is determined by

$$F_{\text{inel}} = \sum_j b_j (\vec{Q} \cdot \vec{\xi}_j) e^{i\vec{Q} \cdot \vec{r}_j}, \quad (5)$$

where b_j is the scattering length of j th atom at \vec{r}_j ,

TABLE I. Atomic shifts in tetragonal PbTiO_3 in units of c . Model (II) assumes that the center of mass is not displaced. The notations, S_1 and S_2 , are used here in a somewhat different way from those in Ref. 11.

	(I)	(II) = $S_1 + S_2$	S_1	S_2
Pb	0	-0.024	0	-0.024
Ti	0.040	0.016	-0.036	0.052
O	0.112	0.088	0.036	0.052

and $(m_j)^{1/2} \xi_j$ is the polarization vector. In the cubic phase, it was not possible to measure the intensity at $q = 0$ accurately for reasons mentioned previously. The comparison was made at $\xi = 0.20$. This relatively high q value was selected to avoid an intensity anomaly due to the mode interaction as described in Sec. IV. It is difficult to assess the reliability of the extrapolation to $q = 0$. Nevertheless, a qualitative agreement (within $\pm 25\%$) was obtained between observed and calculated intensities at the (330), (220), (331), and (003) zones by assuming that ξ_j is proportional to $S_1 + S_2$ given in Table I. Rough estimates of intensities of $q = 0$ mode at (330) and (220) are also in qualitative agreement.

In the tetragonal phase at room temperature, much more definitive measurements can be done because the soft modes are undamped. Lowest transverse branches were measured in the tetragonal phase along two principal directions with the results shown in Fig. 5. Two phonon energies at $q = 0$ give rise to the anisotropy of the dielectric constants ϵ_c and ϵ_a . Previous infrared study by Perry *et al.*¹² gave the lowest optic mode as 83

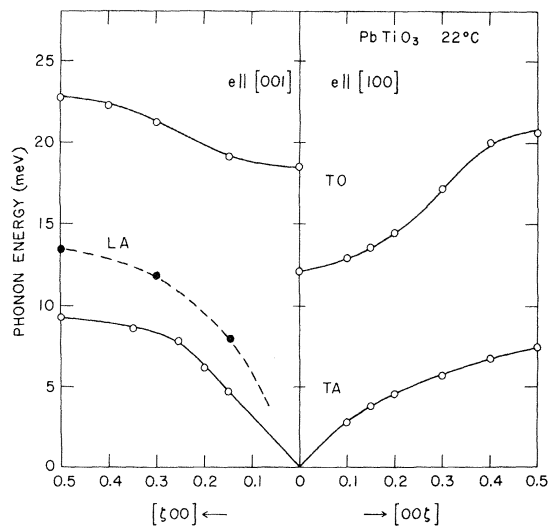


FIG. 5. Phonon dispersion relation obtained for the $(h0l)$ zone of PbTiO_3 . The major part of errors was the result of the nature of "composite" crystal (see text) and estimated to be 0.3-0.7 meV.

TABLE II. Soft-mode intensities of PbTiO_3 at 22°C in the tetragonal phase. Calculations are based upon the displacements of Table I (with the crystal temperature factor of $B=0.57 \text{ \AA}^2$) and scaled to (004).

$(h0l)$	I_{obs}	$S_1 + S_2$	I_{calc} S_1	S_2
200	6 ± 1	6	17	2
300	6 ± 1	4	7	2
400	16 ± 2	19	57	7
301	7 ± 2	4	1	8
002	11 ± 3	8	16	6
003	< 2	1	5	0
004	37 ± 6	37	37	37
103	< 2	2	3	3

cm^{-1} (10.3 meV) in reasonable agreement with the present result.

Intensity measurements of soft modes were carried out at several zone centers with the results shown in Table II together with the calculated values. Measurements were done on the "composite" crystals and may contain some uncertainty due to misalignment. We consider that the agreement is sufficiently good to support our assumption that the tetragonal ionic shifts, with the c. m. condition, correspond to the soft-mode motions.

We can now examine the relation between the dielectric and lattice dynamical parameters. It was shown by Cochran^{4, 13} that

$$C = 4\pi \hbar^2 (v P_s^2 / A_f \sigma) , \quad (6)$$

where v is the unit-cell volume and P_s is the spontaneous polarization. The Curie constant C and

TABLE III. Dielectric and lattice dynamical parameters for BaTiO_3 and PbTiO_3 . The data for BaTiO_3 were quoted by Cochran (Ref. 13). References for PbTiO_3 data are given in the text. The Curie constant C_{calc} was calculated by Eq. (6).

	BaTiO_3	PbTiO_3
$P_s (\mu\text{C}/\text{cm}^2)$	26	57
$A_f (\text{meV}^2/\text{deg})$	0.28	0.13
$\sigma (\text{amu } \text{ \AA})$	0.39	8.14
$C (10^5 ^\circ\text{C})$	1.5 ± 0.3	4.1
$C_{\text{calc}} (10^5 ^\circ\text{C})$	1.2	0.6

A_f were defined in Eqs. (1) and (2), respectively. The ionic shifts δ 's define σ by $\sigma = \sum_j m_j \delta_j^2$. The Curie constants calculated by this equation are given in Table III for BaTiO_3 and PbTiO_3 . As shown by Cochran,¹³ the agreement is good for BaTiO_3 and this may be regarded as a support for the displacive-type transition. On the other hand, the agreement is not satisfactory for PbTiO_3 . However, it may be premature to attribute this poor agreement to the present lattice dynamical model until further experimental confirmation is given to the pertinent data. For example, the previous dielectric study by Bhide *et al.*¹⁴ gave $C = 1.1 \times 10^5 ^\circ\text{C}$. The value of P_s may increase by further refinement of measurement techniques.

ACKNOWLEDGMENTS

We would like to thank J. F. Scott and A. M. Glass for many stimulating discussions and E. M. Kelly for help in crystal growth.

*Work performed under the auspices of the U. S. Atomic Energy Commission.

¹G. Shirane and S. Hoshino, J. Phys. Soc. Japan **6**, 265 (1951).

²G. Shirane, R. Pepinsky, and B. C. Frazer, Acta Cryst. **9**, 131 (1956).

³J. P. Remeika and A. M. Glass, Mater. Res. Bull. **5**, 37 (1970).

⁴W. Cochran, Advan. Phys. **9**, 387 (1960).

⁵M. DiDomenico, Jr., S. H. Wemple, S. P. S. Porto, and R. P. Bauman, Phys. Rev. **174**, 522 (1968).

⁶Y. Yamada, G. Shirane, and A. Linz, Phys. Rev. **177**, 848 (1969).

⁷Useful information on pyrolytic graphite crystals was

given by T. Riste and K. Otnes, J. Nucl. Inst. Methods **75**, 197 (1969).

⁸R. A. Cowley, Phys. Rev. **134**, A981 (1964).

⁹G. Shirane, R. Nathans, and V. J. Minkiewicz, Phys. Rev. **157**, 396 (1967).

¹⁰J. D. Axe, J. Harada, and G. Shirane, Phys. Rev. B **1**, 1227 (1970).

¹¹J. Harada, J. D. Axe, and G. Shirane, Acta Cryst. (to be published).

¹²C. H. Perry, B. N. Khanna, and G. Rupprecht, Phys. Rev. **135**, A408 (1964).

¹³W. Cochran, Advan. Phys. **18**, 157 (1969).

¹⁴V. G. Bhide, K. G. Deshmukh, and M. S. Hegde, Physica **28**, 871 (1962).